Available online at www.sciencedirect.com

SCIENCE DIRECT®

Physics of the Earth and Planetary Interiors 157 (2006) 55–71

PHYSICS OF THE EARTH AND PLANETARY INTERIORS

www.elsevier.com/locate/pepi

Modelling the effects of internal heating in the core and lowermost mantle on the earth's magnetic history

S.O. Costin, S.L. Butler*

Department of Geological Sciences, University of Saskatchewan, 114 Science Place, Saskatoon, Sask., Canada S7N 5E2

Received 29 September 2005; received in revised form 14 March 2006; accepted 17 March 2006

Abstract

Recently, an incompatible-element enriched reservoir, bearing a high degree of radioactive heating, has been proposed to exist at the base of the mantle. This scenario has been discussed based on parameterized thermal and magnetic models of the core [Buffett, B.A., 2002. Estimates of heat flow in the deep mantle based on the power requirements for the geodynamo. Geophys. Res. Lett. 29(12), 7], as well as on geochemical grounds [Tolstikhin, I., Hofmann, A.W., 2005. Early crust on top of the Earth's core. Phys. Earth Plan. Int., 148, 109-130; Boyet M., Carlson, R.W., 2005. ^{142}Nd Evidence for early (> 4.53 Ga) global differentiation of the sillicate earth. Science 309, 576-581]. A high degree of radioactivity at the base of the mantle [Buffett, B.A., 2003. The thermal state of Earth's core. Science 299, 1675-1677], or alternatively the presence of radioactivity in the core [e.g., Labrosse, S., 2003. Thermal and magnetic evolution of the Earth's core. Phys. Earth Plan. Int. 140, 127-143; Nimmo F., Price, G.D., Brodholt, J., Gubbins, D., 2004. The influence of potassium on core and geodynamo evolution. Geophys. J. Int. 156, 363-376], have been proposed as means to allow sufficient buoyancy to power the geodynamo and maintain a magnetic field throughout most of the Earth's history as palaeomagnetic records indicate [McElhinny, M.W., Senanayake, W.E., 1980. Paleomagnetic evidence for the existence of the geomagnetic field 3.5 Ga ago. J. Geophys. Res. 85, 3523-3528; Hale, C.J., D.J. Dunlop, 1984. Evidence for an early Archean geomagnetic field: a paleomagnetic study of the Komati Formation, Barberton Greenstone Belt, South Africa. Geophys. Res. Lett. 11, 97-100], while maintaining a sufficiently high temperature in the core. The present paper analyzes the consequences of internal heating in the core and the lowermost mantle on the core's magnetic history using numerical simulations of convection in the mantle coupled to an energy balance model for the core. This method allows feed-back at each time step between the cooling histories in the core and mantle through the heat flux and temperature at the core-mantle boundary (CMB). We employ a two dimensional, spherical-axisymmetric model of convection in the Earth's mantle, coupled to a heat reservoir model for the core. We calculate at each time-step the entropy available for ohmic dissipation in the core and use this result to estimate the intensity of a magnetic field generated by geodynamo action. In agreement with Nimmo et al. [Nimmo F., Price, G.D., Brodholt, J., Gubbins, D., 2004. The influence of potassium on core and geodynamo evolution. Geophys. J. Int. 156, 363-376], we find that the presence of 300 ppm potassium in the core allows for a magnetic field to have existed over the lifetime of the Earth with a reasonable final value for the temperature at the CMB. Almost all of the models with high internal heating at the base of the mantle exhibit warming of the core throughout much of the Earth's thermal history, a state that would prohibit a functioning geodynamo. In one simulation, we are driven to a scenario where the inner core has existed over the lifetime of the Earth only to gradually melt and then refreeze, with a functioning geodynamo existing for a short time. We conclude that careful tuning of the mantle viscosity, internal heating rate and initial core temperatures would be required in order to achieve a magnetic field over the lifetime of the Earth in

* Corresponding author. Tel.: +1 306 966 5702; fax: +1 306 966 8593.
E-mail address: sam.butler@usask.ca (S.L. Butler).

doi:10.1016/j.pepi.2006.03.009

the presence of a basal layer with a high degree of internal heating and therefore such a scenario must be better constrained before it could present itself as viable.

Keywords: Mantle; Core; Geodynamo; Thermal history; Magnetic field; Radioactivity

1. Introduction

The Earth's magnetic field is generated in the metallic core by dynamo action (e.g., Stevenson, 2003a). Convection of the molten iron alloy in the outer core supplies the energy for the geodynamo process. The buoyancy forces which drive convection in the outer core can be both thermal and compositional. Thermally-driven convection occurs as a result of secular cooling of the core from above. Internal heating in the core, if it exists, adds further thermal buoyancy. When the temperature at the center of the Earth drops below the liquidus for the core alloy, the inner core starts to freeze and inner core solidification proceeds as the core continues to cool. Although the latent heating and gravitational energy release associated with the solidification of the inner core are relatively modest compared with the energy of secular cooling, the compositional buoyancy associated with the release of lighter material from the metallic alloy as the inner core freezes can be a dominant contributor to the geodynamo action.

The cooling of the core and the solidification of the inner core are controlled by the amount of heat the mantle is able to remove from the core. The efficiency with which the mantle extracts heat from the core depends on the temperature drop across the CMB and the dynamical state of convection in the mantle. If the amount of heat extracted from the core is large, vigorous convection takes place in the core, and the geodynamo process can generate a magnetic field and maintain it against dissipative processes. Conversely, if the heat flux across the CMB is too low, the core adiabatic gradient cannot be sustained by the low rate of cooling and the heat transfer is done solely through conduction. In this case, the geodynamo process shuts off. The criterion for a dynamo in terrestrial planets may not differ significantly from the criterion for convection (Stevenson, 2003a), however from entropy considerations it might be concluded that the amount of heat flow across the CMB required to maintain the geodynamo must be in excess of the minimum amount required for convection. Clearly, additional energy sources in the core, such as those associated with the inner core solidification, or internal heating, increase the chances of an operating geodynamo. Thus, the age of the inner core and the heat sources present in the core are of interest for the history of magnetic field generation.

In contrast with geochemical studies which predict an inner core age in excess of 3.5 Gyrs (Brandon et al., 2003), thermal studies for the age of the inner core using parameterized models with prescribed fluxes (e.g., Labrosse et al., 2001; Buffett, 2002), parameterized models of the Earth's thermal history, (e.g., Nimmo et al., 2004), and numerical models of convection coupled with parameterized models for the core (e.g., Butler et al., 2005), have found that the inner core is unlikely to have existed over the entire lifetime of the Earth, its age being probably of order 1.5 Gyrs. The experimental work of Aurnou et al. (2003) and the numerical modeling of Aubert (2005) have also shown that rapid inner core growth, or a young inner core, is consistent with the buoyancy flux at the CMB required to drive polar vortex motions at the CMB that are similar in magnitude to those inferred from the present-day secular variation of the magnetic field (e.g., Olson and Aurnou, 1999). Labrosse et al. (2001), Nimmo et al. (2004), Butler et al. (2005) have all shown that including radioactivity in the core has only a small effect on the age of the inner core. Butler et al. (2005) showed that constraining the inner core growth such that in the final stage the size of the current Earth's inner core is achieved, the age of the inner core can even be decreased slightly by the inclusion of internal heat sources.

The dependence of the power available for the geodynamo process on the heat flow across the CMB has been addressed in a large number of papers (e.g., Buffett et al., 1996; Buffett, 2002; Labrosse and Macouin, 2003) although the exact magnitude of the heat flow at the CMB required to maintain an active dynamo remains poorly constrained. Buffett (2002), Lister (2003), Labrosse (2003) have shown in their energy balance calculations that if ohmic dissipation in the core is required to be the same before and after the appearance of the inner core and the current heat flow at the CMB is required to be reasonably high, as the estimated temperature drop across the CMB of roughly 1000 K suggests (e.g., Anderson, 2002; Boehler, 2000), then unrealistically high early temperatures for the core and mantle are predicted. For models that are integrated forward in time, this result can be restated that if a reasonable initial core temperature is assumed, then models that produce a significant amount of ohmic dissipation throughout their history will have a final core temperature that is likely to be too low. Labrosse (2003) showed, however, that if the amount of ohmic dissipation just before the onset of the solidification of the Earth's core is decreased by an amount within the bounds set by palaeomagnetic studies, much of this problem could be alleviated. A further possibility is suggested by the numerical experiments of Christensen and Tilgner (2004) who utilize results of the Karlsruhe dynamo experiment (Stieglitz and Müller, 2001) to conclude that the heat flow necessary to sustain the dynamo is relatively small. This would require a mechanism to reduce the heat flow from the core to the mantle even with a large temperature drop between the core and mantle, such as a region of high internal heating at the base of the mantle as suggested by Buffett (2002).

In this contribution we analyze the consequences of the presence of radioactive sources in the core or at the base of the mantle, as possible scenarios that have been brought forth to reconcile the geodynamo power requirements with a realistic thermal history in the core. The presence of a heat source in the Earth's core in the form of ^{40}K is inferred from recent high pressure analyses, which indicate that potassium may alloy with iron in a strongly temperature-dependent fashion (Murthy et al., 2003; Lee and Jeanloz, 2003; Gessmann and Wood, 2002), although there remain strong geochemical arguments against large concentrations of potassium in the core (e.g., McDonough, 2004).

At the same time, recent high-precision measurements of samarium-neodymium isotopic data for chondritic meteorites suggest that most of the bulk silicate Earth (BSE) reflects a non-chondritic Sm/Nd ratio; a chondritic BSE for these isotopes could be accounted for if a differentiation event took place within the first 30 million years of the Earth's formation, possibly resulting in a complementary reservoir located at the base of the mantle (Boyet and Carlson, 2005). Arguments for an early-isolated, incompatible-element-bearing reservoir also come from global geochemistry studies on rare gases (Tolstikhin and Hofmann, 2005). The enriched layer would contain radioactive elements (U, Th, K) in excess of the BSE of 20% (Tolstikhin and Hofmann, 2005) to approximately 40% (Boyet and Carlson, 2005), leading to 4–9 TW heat production. The early-formed, enriched, layer envisaged in these studies is quite small, of the order of the seismically imaged D′′ region, and has a very limited mass exchange with the rest of the mantle due to its enrichment in Fe which would make it compositionally denser than the overlying material. Increased radiative thermal conductivity of perovskite and ringwoodite with pressure (Badro et al., 2004; Keppler and Smyth, 2005) and the resulting enhanced radiative heat transfer might also be a mechanism that would result in a long-lived layer at the base of the mantle that has not efficiently participated in producing rocks sampled at the Earth's surface. The early-isolated reservoir could be present at least locally at the base of the mantle, as increased resolution in seismic tomography studies allow for lateral complexity in the lowermost mantle, with possible regions of partial melt (e.g., Williams and Garnero, 1996; Russell et al., 1998). A chemically heterogeneous layer at the base of the mantle could also be the cause of the ultra-low velocity zone seen in D′′ (Lay et al., 1998). Coltice and Ricard (1999) also proposed a layer that is enriched in heat producing elements at the base of the mantle that was the result of the separation of subducted oceanic crust that grows over time. However, the possibility remains that the isotopic anomalies have not been preserved through the Earth's history, as the convective velocities in the mantle may have been an order of magnitude larger at 3.5 Ga (Stevenson, 2003b).

Previous studies of Earth's geodynamo power requirements generally used prescribed heat flux across the CMB or parameterized models for the energetics of the core and the mantle. The present paper calculates the entropy production in the outer core as a function of time based on numerical simulations output for mantle convection. Further, the Earth's magnetic evolution is modelled based on the ohmic dissipation in the outer core. Coupling the global energy balance in the core with fully dynamical mantle models was first employed by Steinbach et al. (1993). Using a similar approach, Stegman et al. (2003) explored the possibility of an early lunar dynamo. Nakagawa and Tackley (2005) used thermochemical mantle simulations in order to analyze the thermal evolution of the core and the implications for magnetic history and they found that 100 ppm potassium in the core as well as a dense layer accumulating at the base of the mantle best explained the Earth's magnetic and thermal history.

In our model, we compute the energy balance and entropy production in the core as a function of the heat flow and temperature at the CMB at each time step in the numerical simulation, allowing therefore a complete feed-back between the dynamic processes in the core and mantle. As we shall present in the following sections, coupling the cooling history of the core and the inner core growth model with the thermal history of the mantle, which accounts for temperature-dependent viscosity, internal heating and layering, yields results difficult to predict from parameterized models, as short time-scale mantle events, which are not captured by parameterized models, can considerably affect the thermal and magnetic history in the core. In addition, the use of the numerical model allows us to investigate the effects of laterally varying mantle properties.

In the following, we outline our model for calculating the entropy available for ohmic dissipation from the output of our numerical mantle convection model. In subsequent sections, we present the results for a nominal simulation and then discuss the effects of internal heating in the core and internal heating in a basal layer in the mantle.

2. Model description

We employ the core thermal model and the numerical model of convection in the Earth's mantle described in Butler et al. (2005) which we will outline briefly in the following two sections. In Section 2.3, we present the approach used to estimate the vigor of the geodynamo from the entropy of ohmic dissipation.

2.1. Mantle model

The mantle model is based on the model originally developed by Solheim and Peltier (1994a,b) and modified by Butler and Peltier (2000). The model employs radially dependent thermodynamic and transport properties that are fit to be as Earth-like as possible. The viscosity in the mantle is radially dependent and is dependent on the average temperatures in the lower and upper mantle as described in Butler et al. (2005). The internal heating rate in the mantle varies as a function of time. Following Hart and Zindler (1986), the uranium/thorium/potassium ratio is taken to be 1/4/10000 and the final internal heating rate in the mantle is scaled to be 13 TW . When there is a region of high internal heating at the base of the mantle, it is assumed to have the same proportion of radioactive elements concentrated in the lowermost 200 km of the mantle and the heat sources are immobile. We do not impose any sort of barrier to flow or viscosity variation at the region of high internal heating at the base of the mantle. The temperature at the lower boundary of the convecting mantle is the CMB temperature and it varies as a function of time but is spatially uniform.

2.2. Core thermal model

It is generally assumed that vigourous convection in the core maintains a well-mixed, adiabatic mean state in the core. The global heat conservation in the core states that the total heat loss of the core, which equals the heat flux at the core-mantle boundary ($Q_{\rm cmb}$), is balanced by the sum of the heat sources in the core (Buffett et al., 1992; Lister and Buffett, 1995; Buffett, 2002; Labrosse, 2003; Gubbins et al., 2003; Nimmo et al., 2004)

$$Q_{\rm cmb} = \chi_{\rm sec} + \chi_{\rm L} + \chi_{\rm G} + \chi_{\rm r}, \tag{1}$$

where $\chi_{\rm sec}$, $\chi_{\rm L}$, $\chi_{\rm G}$, $\chi_{\rm r}$ represent the rates of secular cooling of the core, latent heating and gravitational energy release due to the growth of the inner core, and internal heating in the core, respectively. Using (1) and the definition of secular cooling, the temperature at the CMB is updated at each time step of the mantle convection model as follows

$$\frac{{\rm d}T_{\rm cmb}}{{\rm d}t} = \frac{-Q_{\rm cmb} + \chi_{\rm r} + \chi_{\rm L} + \chi_{\rm G}}{C_{\rm pc}}. \tag{2}$$

Here, $T_{\rm cmb}$ is the temperature at the core mantle boundary, $C_{\rm pc} = 1.5 \times 10^{27}$ J/K is the adiabat-weighted, effective heat capacity of the core (Butler et al., 2005). The heat flow across the CMB, $Q_{\rm cmb}$, is evaluated from the temperature gradient and the thermal conductivity at the base of the model mantle. It is assumed that convection in the mantle controls the rate of heat loss from the core.

The rates of latent heat and gravitational potential energy release are proportional to the rate of inner core growth and are expressed by (Stacey, 1992)

$$\chi_{\rm L} = 4\pi \mathcal{L} \rho_{\rm ic} r_{\rm ic}^2 \frac{{\rm d}r_{\rm ic}}{{\rm d}t}, \tag{3}$$

$$\chi_{\rm G} = \frac{8\pi^2}{15} G \Delta\rho_{\rm icb} \rho_{\rm c} (3\, r_{\rm cmb}^2 r_{\rm ic}^2 - 5 r_{\rm ic}^4) \frac{{\rm d}r_{\rm ic}}{{\rm d}t}. \tag{4}$$

In (3) and (4), $\mathcal{L} = 8 \times 10^5$ J/kg is the latent heat of freezing of core material (Buffett et al., 1996), $\rho_{\rm c} = 1.1 \times 10^4\,{\rm kg/m^3}$ and $\rho_{\rm ic} = 1.27 \times 10^4\,{\rm kg/m^3}$ (Stacey, 1992) are the mean densities of the inner and outer core, and $\Delta\rho_{\rm icb} = 400\,{\rm kg/m^3}$ is the density drop across the inner core boundary (ICB) associated with the presence of a light element in the core (Buffett et al., 1996). The notations $r_{\rm ic}$ and $r_{\rm cmb}$ represent the radii of the ICB and CMB, respectively, while G is the gravitational constant. The radius of the inner core is calculated from

$$r_{\rm ic}(t) = \left(\frac{T_{\rm L}(0) - \Gamma T_{\rm cmb}(t)}{\Lambda} \right)^{1/2}. \tag{5}$$

Here, $T_{\rm L}(0)$ is the liquidus temperature at the center of the core which is taken to be 5700 K (Anderson, 2002). The parameter Γ represents the fractional increase in the adiabatic temperature from the CMB to the ICB, while

$$\Lambda = \frac{2\pi}{3} G \rho_{\rm ic}^2 \frac{{\rm d}T_{\rm L}}{{\rm d}P}, \tag{6}$$

parameterizes the variation of the core liquidus with radius (P is pressure). The value of Γ is assumed constant for a given simulation and is chosen by iterating the solutions over the lifetime of the inner core until an inner core with an Earth-like radius is achieved, as described in Butler et al. (2005). In most of the calculations, the liquidus parameter, Λ, is kept unchanged, however this quantity was varied in runs D1 and D3 since it was not found to be possible to obtain an Earth-like final value of the inner-core size by varying the core adiabat parameter, Γ, alone. All of the values used for Λ and Γ are listed in Table 1. It is particularly important to finish with an Earth-like inner core for calculations of the entropy of ohmic dissipation since latent heating and especially the release of gravitational potential energy have a dominant contribution to the entropy budget once an inner core starts to form.

2.3. Entropy calculation

The global energy balance stated in Section 2.2 relates the heat flux across the CMB to the heat sources in the core. However, it does not account for the magnetic energy, because, physically, the magnetic energy is both generated and dissipated internally in the core and therefore does not affect the heat balance (Gubbins et al., 2003). Since the magnetic energy can be related to the dissipative processes, one way to estimate the energy available for regeneration of the magnetic field is to examine the entropy production in the core and assess the contribution given by dissipation, which in turn will clue us into the available energy to drive the geodynamo. In the outer core, dissipation is dominated by Joule heating (e.g., Labrosse, 2003), and only a small fraction ($\approx$ 2–5% of the total dissipation) occurs through viscous dissipation, because electrical resistance dominates viscosity in its dissipative effects in a highly conductive material such as the iron alloy (Gubbins et al., 2003).

The entropy contributions in the core are determined by dividing each of the heat sources by the temperature at which they are supplied. For a heat engine working in an 'ideal' Carnot-cycle, if the temperature at which the input heat is provided (say, $\mathcal{T}_+$) is higher that the temperature at which heat is extracted ($\mathcal{T}_-$), the efficiency of the engine to do useful work is computed as $\eta = 1 - \frac{\mathcal{T}_-}{\mathcal{T}_+}$ (Braginsky and Roberts, 1995). In a global entropy budget for the core, the entropy at the CMB equals the sum of entropy sources within the core, including the entropy given by the dissipation term, integrated over the volume of the core

$$\frac{Q_{\rm cmb}}{T_{\rm cmb}} = -S_{\rm adb} - S_{\rm ohm} + \frac{\chi_{\rm r}}{\bar{T}_{\rm c}} + \frac{\chi_{\rm sec}}{\bar{T}_{\rm c}} + \frac{Q_{\rm icb}}{T_{\rm icb}}. \qquad (7)$$

Here, $S_{\rm adb}$ is the entropy created by thermal conduction down the adiabatic gradient in the core, while the remaining terms on the right hand side represent the entropy due to ohmic dissipation, internal heating, secular cooling, and the entropy created at the inner core boundary.

We assume that the radiogenic sources in the core, if present, are uniformly distributed throughout the core. At the same time, the secular cooling of the core, which is usually the largest heat source in the core, also occurs uniformly throughout the core. Therefore, to compute the entropy given by these two heat sources, we divide these heat sources by the mean temperature in the core, $\bar{T}_{\rm c}$. Similarly, we make the assumption that the entropy given by dissipation is effectively produced at the mean temperature in the core, since it ultimately reflects the production of magnetic energy, which is the work done by the heat engine. An additional argument follows from

Table 1
Run summary

Model name	$\chi_{\rm c}(t^p)$ (TW)	$\chi_{\rm lm}(t^p)$ (TW)	$\chi_{\rm m}(t^p)$ (TW)	$T_{\rm cmb}(t(0))$ (K)	Λ (K m^{-2})	Γ	$\Gamma_{\rm mean}$	η_0	Cov
B0	0	0	13	4300	1.6526×10^{-10}	1.556	1.20	1	1
B1	1	0	13	4300	1.6526×10^{-10}	1.46	1.17	1	1
B2	2	0	13	4300	1.6526×10^{-10}	1.3915	1.1456	1	1
B4	4	0	13	4300	1.6526×10^{-10}	1.26	1.1	1	1
D1	0	13	0	4300	9.8798×10^{-11}	1.2759	1.105	1	1
D2	0	13	0	4300	1.6526×10^{-10}	1.2373	1.090	1	0.5
D3	0	13	0	4300	1.2770×10^{-10}	1.3108	1.117	0.5	1
D4	0	13	13	4300	1.6526×10^{-10}	1.3435	1.1288	1	1
D5	0	4	13	4300	1.6526×10^{-10}	1.4838	1.177	1	1
H1	0	0	26	4300	1.6526×10^{-10}	1.5617	1.203	1	1

The symbols $\chi_{\rm c}(t^p)$, $\chi_{\rm lm}(t^p)$ and $\chi_{\rm m}(t^p)$ represent the prescribed internal heating rates in the core, lowermost 200 km of the mantle, and mantle at modern times. $T_{\rm cmb}(t(0))$, Λ, Γ, are the initial temperature at the CMB, the core liquidus parameter, adiabat parameter, and mean temperature parameter. η_0 and Cov are the initial viscosity multiplier and the fractional azimuthal coverage of the region of high internal heating in the lowermost mantle.

the fact that as the 'ideal efficiency' of the engine cannot be exceeded, the dissipation must occur at such a temperature T_D, that $T_{cmb} \leq T_D \leq T_{icb}$ (Braginsky and Roberts, 1995).

The heat produced at the inner core boundary is due to the secular cooling of the inner core and the latent heat released by the freezing of the inner core. For simplicity, we incorporate the secular cooling of the inner core into the general secular cooling term. The other heat source that creates entropy at this horizon is the latent heat due to the crystallization of the inner core. The latent heat is similar to the specific heat, in that when the core cools by a small amount, the freezing releases heat concentrated at the ICB (Gubbins et al., 2003).

Using (7) and (1), the entropy available for ohmic dissipation, S_{ohm}, can be written in terms of the various heat flows and heat sources present in the outer core

$$S_{ohm} + S_{adb} = S_r + S_{sec} + S_L + S_G. \tag{8}$$

Here, S_r, S_{sec}, S_L and S_G represent the various contributions to the entropy of dissipation from internal heating, secular cooling, latent heating and gravitational energy release, respectively. Employing the quantities calculated in the core model, these terms take on the following forms

$$S_{adb} = \frac{16\pi}{5} r_{cmb} k_c (\ln \Gamma)^2, \tag{9}$$

$$S_r = \frac{\chi_r}{T_{cmb}}\left(1 - \frac{1}{\Gamma_{mean}}\right), \tag{10}$$

$$S_{sec} = \frac{\chi_{sec}}{T_{cmb}}\left(1 - \frac{1}{\Gamma_{mean}}\right), \tag{11}$$

$$S_L = \frac{\chi_L}{T_{cmb}}\left(1 - \frac{1}{\Gamma}\right), \tag{12}$$

$$S_G = \frac{\chi_G}{T_{cmb}}, \tag{13}$$

where we have defined Γ_{mean} such that the mean temperature in the core can be expressed as a function of the numerical output T_{cmb}, i.e., $\bar{T}_c = \Gamma_{mean} \times T_{cmb}$. Further,

$$\Gamma_{mean} = \frac{3}{4 \ln \Gamma}\left[\Gamma \left(\frac{\pi}{\ln \Gamma}\right)^{0.5} Erf[(\ln \Gamma)^{0.5}] - 2\right] \tag{14}$$

is calculated assuming a Gaussian adiabatic temperature profile in the core (e.g., Nimmo et al., 2004; Labrosse et al., 2001) and is always less than Γ. Here, k_c represents the thermal conductivity of the core, which we take to be 36 W/(m K) (Buffett et al., 1996). For consistency, S_{adb} has also been calculated assuming a Gaussian adiabatic temperature profile in the core.

Physically, the entropy equation (8) states that the dissipative processes and the heat conducted down the adiabat must be sustained from the entropy production of various heat sources in the core. For a detailed derivation of the entropy available for ohmic dissipation the interested reader is also referred to Labrosse (2003), Gubbins et al. (2003).

The changes in entropy arising from different sources and sinks appear in (8) in the same way as if evaluated by the Carnot cycle of a heat engine working over an adiabatic temperature range (Braginsky and Roberts, 1995; Stacey, 1992, p. 306): each heat source is multiplied by an efficiency factor which depends on the temperature at which the respective heat source is supplied. Consequently, the secular cooling and the radioactive heating enter the entropy equation with a small efficiency $1/T_{cmb}(1 - 1/\Gamma_{mean})$, since these heat sources are distributed over the whole core (Labrosse and Macouin, 2003), whereas the entropy produced by the latent heat released at the ICB is calculated using the higher efficiency factor $1/T_{cmb}(1 - 1/\Gamma)$. The energy released by the gravitational differentiation at the inner core boundary, although it does not create entropy at the ICB horizon, consists of the work done by the hot, buoyant material at the CMB and therefore enters the entropy balance with a much larger factor, as $1/T_{cmb}$ (Braginsky and Roberts, 1995; Labrosse, 2003; Nimmo et al., 2004). It can also be noted that the effects of core cooling are more significant in the heat balance than in the dissipation, where the compositional terms predominate. It will also be noted that S_{abd} has a constant value throughout each simulation, however, it differs from one simulation to another as Γ is allowed to vary due to the modern-day inner-core radius constraint. As a result, when comparing simulations for which different values of Γ are used, it is often useful to compare the sum of the entropy available for ohmic dissipation and thermal conduction down the core adiabat as a measure of the vigor of geodynamo action.

It is uncertain as to to how much entropy of ohmic dissipation must be available in order for a magnetic field to be present and most likely these minimum conditions are dependent on shell geometry (Heimpel et al., 2005). In what follows, we make a minimal assumption that a magnetic field can be generated if there is positive entropy available for ohmic dissipation. We assume that the field produced in the outer core is proportional to the square root of the ohmic dissipation (i.e. the wavelength spectrum of the magnetic field does not change with time). In these calculations, we are assuming a purely electrically insulating mantle and therefore neglect the ohmic dissipation possibly produced by electric currents that leak from the core and into the mantle (Kuang and Chao, 2003), or by electric currents induced in the lowermost mantle by time-varying fields in the core (Costin and Buffett, 2004). The magnetic history model obtained by scaling the ohmic dissipation represents a crude approximation of the observed field, as the toroidal and poloidal components of the magnetic field in the core may vary independently from one another. However, the model enables us to relate features of the long-term secular variation to the coupled dynamics of the core and mantle. For the sake of comparison, when we plot the magnetic field as a function of time, we normalize the field by the same reference value.

3. Results

In Table 1 we list the various simulations we have performed. The thermal results for the B series models which have varying degrees of internal heating in the core were discussed in Butler et al. (2005). Here we consider the magnetic implications of radioactive potassium in the core. The D series models explore the effects of high concentrations of radioactive internal heat sources in the lowermost 200 km of the mantle, while model H1 is used to explore the effects of high internal heating throughout the mantle. In what follows, we first describe the results from model B0 which has no internal heating in the core and no increased concentration of radioactivity in the lowermost mantle. In subsequent subsections, we explore the effects of increasing the initial core temperature, and the concentrations of radioactive elements in the above-mentioned regions of the Earth. In Section 3.4, we briefly discuss the scaling of the inner-core growth with time.

3.1. A model thermal and magnetic history

Fig. 1 shows the results of our nominal run, B0, which assumes 13 TW (final rate) internal heating in the mantle, no internal heating in the core and starts with an initial CMB temperature of 4300 K. The initial azimuthally averaged radial mantle temperature profile is adiabatic and set such as to be at the solidus temperature of Boehler (2000) for the upper mantle. The initial lateral variations in mantle temperature are taken from a previous convection simulation with a similar effective Rayleigh number.

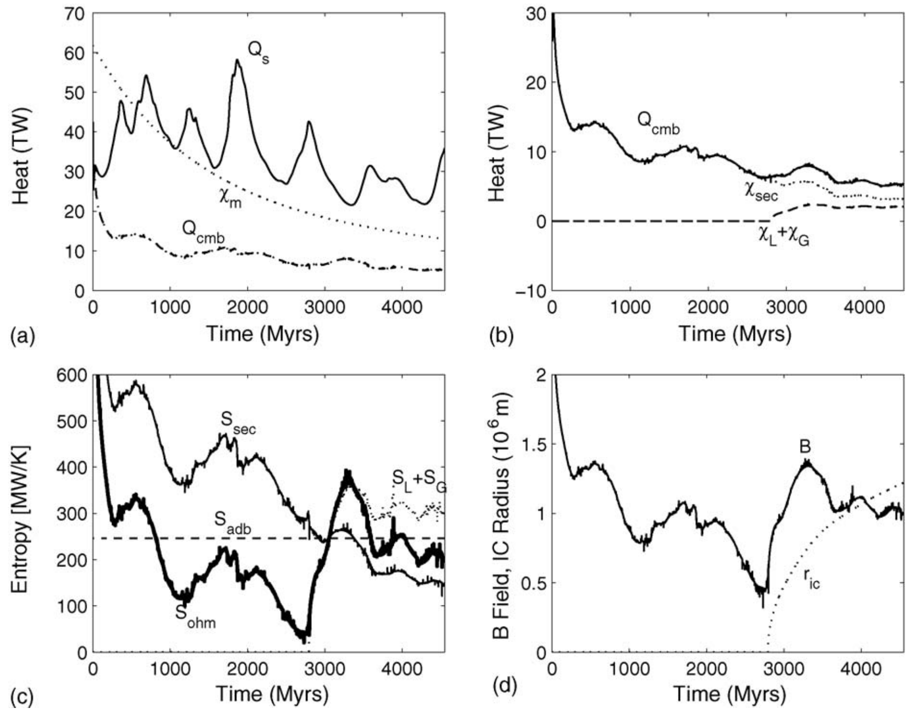

Fig. 1. Results of calculation B0. (a) Time variation of the surface heat flow (solid line), internal heating rate in the mantle (dotted line) and heat flow at the CMB (dashed line). (b) Time variation of the CMB heat flow (solid line), secular cooling rate of the core (dotted line), and sum of the energy release due to latent heating and gravitational energy release associated with the solidification of the inner core (dashed line). (c) Entropy of ohmic dissipation (thick solid line), of secular cooling (thin solid line), associated with conduction down the core adiabat (dashed line) and the sum of the entropy associated with latent heat and gravitational energy release (dotted-line). (d) Normalized magnetic field, and the radius of the inner core.

The same initial mantle temperature distribution is used in all of the simulations. In Fig. 1a we display the heat flow at the Earth's surface (solid line), the internal heating rate in the mantle (dotted line) and the heat flow conducted across the CMB (dashed line).

Because there is no internal heating in the core, secular cooling is the only contribution to the heat flow across the CMB before the onset of inner core growth. As can be seen in Fig. 1b, the secular cooling is quite high, revealing a rapid cooling of the core. As can be noted from Table 2, the final CMB temperature for this case is 3505 K, which is low compared with most estimates for this quantity (e.g., Anderson, 2002; Boehler, 2000). The CMB heat flow exceeds the secular cooling once the inner core starts to form and latent heating and gravitational potential energy release occur. As mentioned earlier, although these are quite small in terms of their contribution to the energy budget of the core, they make the largest contribution to the entropy of ohmic dissipation over the final 1 Gyr of the simulation, as seen in Fig. 1c (dotted line) due to their relatively high efficiency factors. The entropy production due to secular cooling (thin solid line) is very large early on, when the core is cooling rapidly, but declines significantly over the course of the calculation. The entropy of ohmic dissipation (thick solid line) jumps significantly when the inner core begins to form and the contributions of latent heating and gravitational energy release become significant. In Table 2 we list the quantity Σ_{ent}, which we have defined as the ratio of the minimum of $\langle S_{\mathrm{ohm}} + S_{\mathrm{adb}}\rangle$ to the average for this quantity over the lifetime of the inner core, thus giving a measure of the variability of geodynamo power. For this calculation, Σ_{ent} takes on a relatively modest value of 0.54.

It will also be noted that for this simulation, the onset of inner core solidification occurs just before the time when the geodynamo action is about to cease, as S_{sec} drops below S_{adb}. The contribution of $S_{\mathrm{G}} + S_{\mathrm{L}}$ becomes significant just as the secular cooling cannot sustain the adiabatic gradient and therefore makes possible the existence of the geodynamo. However, part of the reason for the dramatic decrease in S_{sec} is the warming of the core due to the effects of inner core solidification. Still, based on the slope of S_{sec} before the onset of inner core solidification, it appears that were the onset of inner core solidification delayed just by a few hundred Myrs, there would have been a period without a magnetic field for this case. We plot the magnetic field normalized by the final value, assumed to represent the modern-day magnetic field. To ease comparison, we retain this final value of the nominal case and employ it to normalize all subsequent results. In Fig. 1d we show the normalized magnetic field, B, and the radius of the inner core as a function of time. The magnitude of the magnetic field displays fluctuations on a large time-scale, and jumps abruptly by a factor of three at the time of onset of inner core solidification, which cannot be ruled out by palaeomagnetic evidence (e.g., Macouin et al., 2004). Smirnov et al. (2003) showed evidence for an increase in the strength of the Earth's magnetic at 2.5 Ga which they attribute to the initiation of inner core growth. It can be observed that the secular variation is largely reflecting the temporal variability in the CMB heat flux. This scenario produces a magnetic field throughout geological time, however, continuous generation of the magnetic field is merely coincidentally realized through the onset of the inner core freezing. In addition, an unrealistic final CMB temperature is rendered.

Table 2
We list the final CMB temperature, $T_{\mathrm{cmb}}(t^p)$, the temporal average entropy of ohmic dissipation $\langle S_{\mathrm{ohm}}\rangle$ and entropy of ohmic dissipation and conduction down the core adiabat $\langle S_{\mathrm{ohm}} + S_{\mathrm{adb}}\rangle$, the ratio of the sum of the minimum entropy of ohmic dissipation and entropy due to the adiabatic gradient to the temporal average of this quantity over the lifetime of the inner core, Σ_{ent}, the total time for which the entropy of ohmic dissipation is positive, t_B, the age of the inner core, the final radius of the inner core, $r_{\mathrm{ic}}(t^p)$ and the best-fitting scaling exponent between inner-core growth and time, α

Model name	$T_{\mathrm{cmb}}(t^p)$ (K)	$\langle S_{\mathrm{ohm}}\rangle$ (MW/K)	$\langle S_{\mathrm{ohm}} + S_{\mathrm{abd}}\rangle$ (MW/K)	Σ_{ent}	t_B (Myrs)	I.C. Age (Myrs)	$r_{\mathrm{ic}}(t^p)$ (km)	α
B0	3505	223	479	0.54	4550	1756	1221	0.406
B1	3736	286	466	0.51	4550	1680	1219	0.483
B2	3921	338.4	476	0.67	4550	1647	1216	0.413
B4	4326	355.5	451	0.66	4550	1482	1228	0.437
D1	4351	−11.2	75	0	2259	2127	1224	0.414
D2	4293	−180	−123	0	1206	4550	1188	–
D3	4201	14.2	106	0	2485	2541	1231	0.482
D4	4050	50.8	160.1	0	2779	2435	1253	0.385
D5	3676	153	341	0	3944	1679	1218	0.519
H1	3499	241	491	0.38	4550	1977	1245	0.363

This calculation illustrates some of the challenges mentioned earlier. The most efficient heat sources in generating magnetic fields are those associated with inner core solidification. It is difficult on thermal grounds to have had an inner core throughout the lifetime of the Earth, however, and it is necessary to drive the geodynamo in a purely thermal manner at early times. This implies that if we require a positive entropy of ohmic dissipation just prior to the formation of the inner core, particularly if we require similar ohmic dissipation before and after the inner core begins to freeze, there must be a large degree of either secular cooling or internal heating in the core. If the degree of secular cooling is large, a high initial core temperature is required in order to avoid a final CMB temperature which is too small. In what follows, we investigate models with internal heating in the core and with high degrees of internal heating in the lowermost mantle.

3.2. *Effects of internal heating in the core*

In Fig. 2 we display the results of simulation B2 with 2 TW of internal heating (final rate) in the core, corresponding to 300 ppm potassium. The heat flow at the CMB is quite high, with a final value of 7.1 TW. At early times the core is warming up due to the presence of the internal heat sources leading to a negative entropy contribution from secular cooling. The entropy associated with internal heating more than makes up for this, however, and as shown in Fig. 2c, the entropy available for ohmic dissipation is fairly constant throughout the entire calculation. It will be noted that secular cooling and internal heating power the dynamo with equal efficiency factors. In this case, there is a relatively small increase in the magnetic field at the time of onset of inner core solidification. The average entropy available for ohmic dissipation over the lifetime of the Earth increases with the degree of internal heating in the core (see Table 2), however, all of this increase can be attributed to the change in the entropy required for the adiabatic gradient. If these terms are summed, the total entropy available for ohmic dissipation and conduction down the adiabat is roughly unchanged with the degree of internal heating in the core. This can be explained by two effects. One effect is that models with high degrees of internal heating have higher core temperatures which decrease the efficiency factors for all of the heat sources and fluxes. The other effect is that as internal heating in the core is increased for models that are otherwise the same, an increasing amount of the heat energy goes into warming the core, decreasing the secular cooling term. A simulation with a higher initial core temperature and 2 TW of internal heating in the core

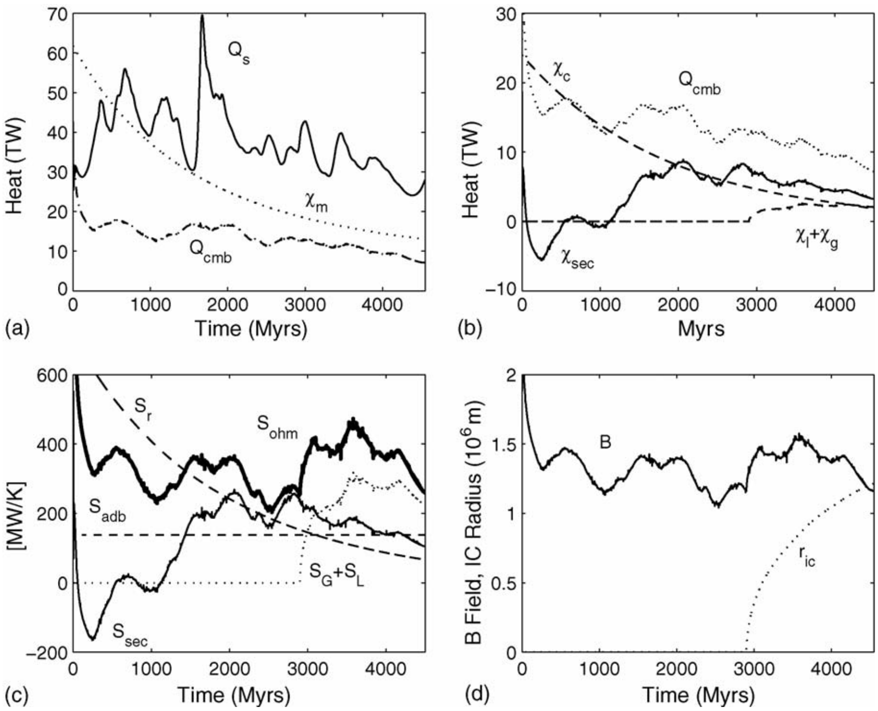

Fig. 2. From calculation B2: (a) mantle heat flows and sources; (b) core heat flows and sources; (c) entropy sources in the core; and (d) normalized magnetic field and the inner core radius.

in the final state (not shown) resulted in a greater degree of core cooling. This indicates that, with an initially hotter core, core internal heating causes a more significant increase in the entropy available for dissipation.

The magnetic field in B2 is present throughout the entire simulation and although it displays some long time-scale variability (of the order of several hundred Myrs), the amplitude of the fluctuations is less than in the nominal case B0, which makes this case a potentially viable scenario for the magnetic evolution. The final magnitude of the magnetic field is also slightly greater than for case B0 as can be seen in Fig. 2 (the final value of B is greater than 1). In one instance, a long period of high magnetic field intensity (between roughly 1.2 and 2.2 Gyrs) is caused by fluctuations in convection in the mantle, whereas as the mantle activity lessens in vigor towards the last 1 Gyrs of the simulation, another period of high magnetic field occurs due to the addition of compositional terms in the entropy balance with the onset of inner core freezing. The high intensity periods are separated by low intensity periods, reminiscent, for instance, of the Mesozoic dipole low (e.g., Tanaka et al., 1995). The interesting feature displayed by the magnetic evolution for this case is the apparent fluctuations about a linear trend, which is more likely supported by palaeomagnetic data, in that the palaeointensities at earlier times in the Earth's evolution have rather shown lower or similar values to the Cenozoic data (e.g., Hale, 1987; Prévot et al., 1990; Macouin et al., 2004).

3.3. *Effects of high internal heating in the lowermost mantle*

In Fig. 3 we display the results of calculation D1 with 13 TW (final rate) of internal heating concentrated in the lowermost 200 km of the mantle. This represents an end-member model, where all of the radioactive heating is concentrated in the lowermost mantle which we know is not exactly the case, but it serves to illustrate a number of features of models of this kind. In this case, it was found necessary to decrease the liquidus parameter, Λ, in order to achieve an Earth-like inner core size. The value of the slope of the liquidus, $\frac{dT_L}{dP}$ implied herein is 4.4×10^{-9} K/Pa, slightly smaller than high pressure physics estimates for this quantity.

For this scenario, heat is flowing from the mantle into the core for roughly the first half of this simulation due to the extremely high concentration of radioactive elements at the base of the mantle. This can also be observed from Fig. 4 where the CMB temperature for model D1 is increasing during this time. As a result, there cannot be a magnetic field until the radioactive heat sources

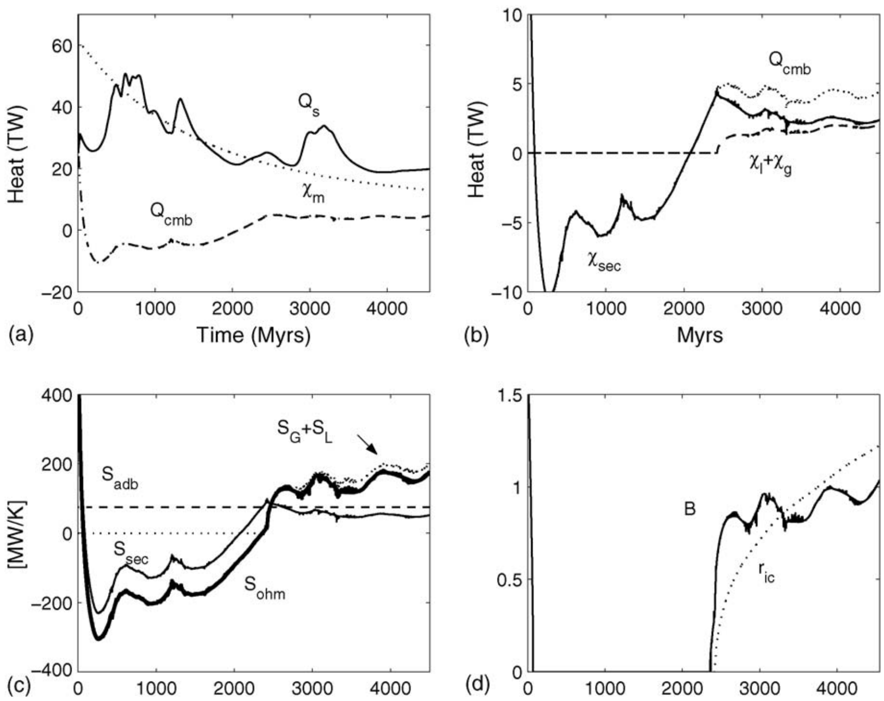

Fig. 3. From calculation D1: (a) mantle heat flows and sources; (b) core heat flows and sources; (c) entropy sources in the core; and (d) normalized magnetic field and the inner core radius.

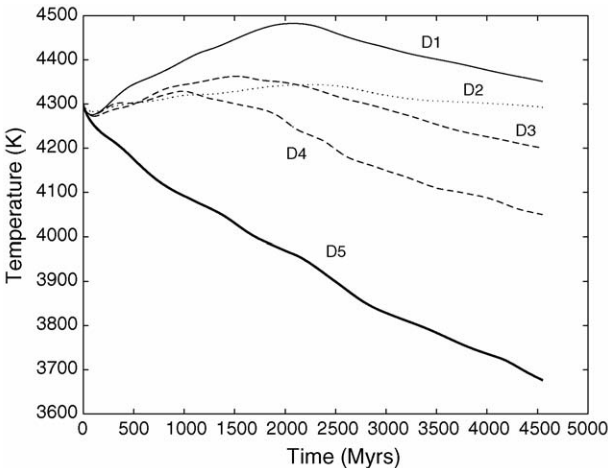

Fig. 4. The evolution of the temperature at the CMB for the various D series models.

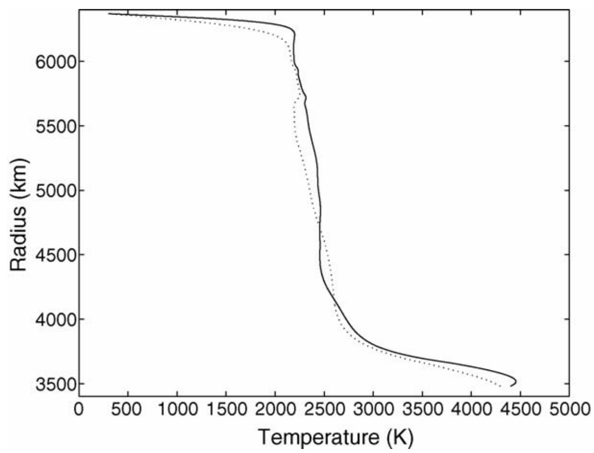

Fig. 5. The geotherm from calculation D1 at times 1000 (solid line) and 4550 Myrs (dotted line).

have diminished to the extent that heat flow at the CMB can reverse direction. In this calculation, this happens at essentially the same time that the inner core begins to form. Therefore, for this case the magnetic history is strongly dependent on the onset and growth of the inner core, which has existed for roughly 2 Gyrs. This scenario might not be plausible for the Earth's case, however, it might explain observations from other terrestrial bodies (e.g., Venus has currently no magnetic field, possibly because its core is not cooling at present, Nimmo, 2002). It must be pointed out that in this calculation, we did not allow for the possibility of an initial inner core that melted and then refroze and we looked only at the effects of a solidifying core during the cooling phase of the simulation. A simulation that includes an initial core that partially melts and refreezes will be discussed below. The data in Table 2 show that the final CMB temperature of 4351 K is actually higher than the initial value and the final CMB heat flow is 4.68 TW.

In Fig. 5 we display the geotherm for this calculation after 1000 Myrs and 4550 Myrs. At the earlier time, the geotherm has a maximum above the CMB implying that heat is flowing both into the core and into the mantle from this hot lower layer. At 4550 Myrs, heat is no longer flowing into the core, but the geotherm still shows a significant degree of curvature in the basal thermal boundary layer which is indicative of the high internal heating rate in that region. This also implies that the heat flow from the lowermost layer into the rest of the mantle is higher than the heat flow at the CMB. In order to arrive at an Earth-like final-sized inner core for this model, both the liquidus parameter and the core adiabat needed to be decreased because of the very small decrease in the temperature of the CMB in the latter half of the calculation.

In Fig. 6 we display the results of calculation D2 with high internal heating in the lowermost 200 km of the mantle over 1/2 of the hemisphere of the core. This simulation is intended to model the effects of laterally heterogeneous internal heating. It must be pointed out that the viscosity in the mantle is allowed to vary only radially and some of the effects of laterally heterogeneous internal heating on mantle heat transport may not be captured in this model. In this calculation, the temperature at the CMB showed very little variation throughout the simulation as can be seen in Fig. 4. This is the result of heat entering the core on the hot part of the CMB and leaving on the cold part. It was not found possible to achieve a correct-sized inner core by means of any reasonable combination of the parameters T_{L0}, Λ and Γ when a model was started with no initial inner core. Hence, the model was started with a primordial inner core of radius of 1171 km. The thermal history in Fig. 6 reveals that except for a very brief initial period of core cooling, heat is flowing from the mantle into the core until roughly 2500 Myrs into the simulation. As a result, the inner core is gradually melting during this period and gradually grows over in the the latter part of the simulation. During the later cooling phase, there is only a period of roughly 1 Gyr when there is sufficient entropy to maintain both ohmic dissipation and conduction down the adiabatic gradient, therefore there is only an episodic, weak, magnetic field throughout the simulation. It will also be pointed out that Glatzmaier et al. (1999) found that geodynamo simulations produce the most Earth-like magnetic fields when the CMB heat flow is close to spatially uniform and Olson and Christensen (2002) demonstrated that geodynamo simulations where the magnitude of the spatial variation is greater than the

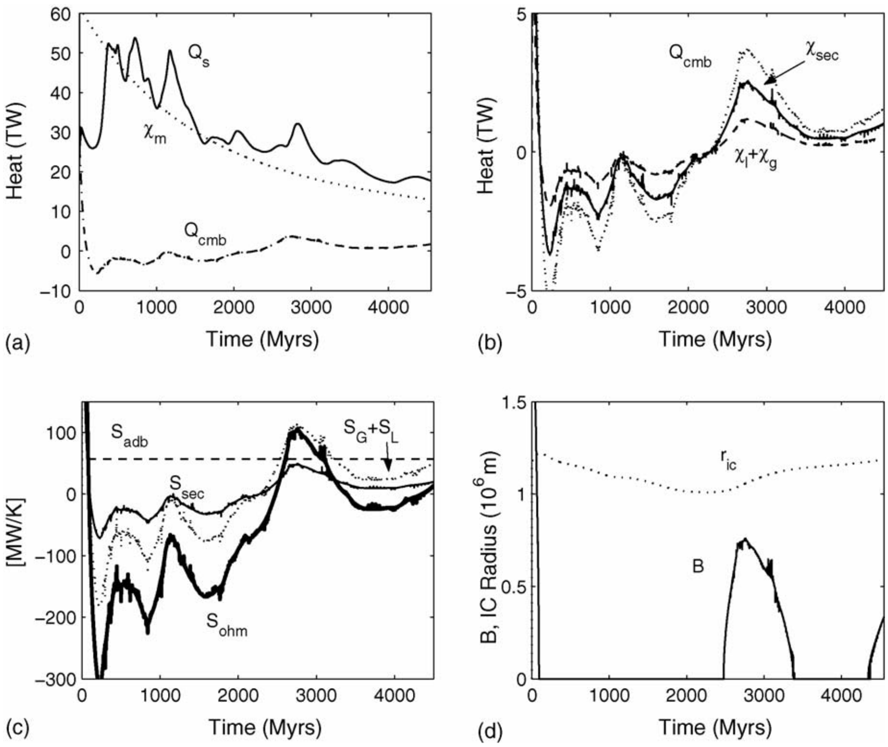

Fig. 6. From calculation D2: (a) mantle heat flows and sources; (b) core heat flows and sources; (c) entropy sources in the core; and (d) normalized magnetic field and the inner core radius.

mean value of the heat flow at the CMB, usually fail to produce a magnetic field. As a result, it is possible, given the very large spatial variations in CMB heat flow in the D2 simulation, that a magnetic field would not have been produced even at times when there is entropy available for ohmic dissipation and if present, it would have had a very strongly non-dipolar character. The short-lived magnetic field is reminiscent of the short-lived early Martian magnetic field (Acuña et al., 1999). In our scenario, the episodic field is driven largely by the compositional terms, in contrast with recent models for the Martian field (Breuer and Spohn, 2006) which indicate a thermally short-lived magnetic field. The final inner core radius is only slightly greater than its initial value, and the CMB temperature is very close to constant throughout this entire simulation. As explained before, part of this is caused by the laterally heterogeneous high internal heating at the base of the mantle. The other factor is that the effects of latent heating/cooling are present throughout this entire simulation which act to increase the effective heat capacity of the core, resulting in reduced variations of the core temperature.

Simulation D3 was run with an identical configuration to model D1 with the exception that the initial viscosity of the mantle was decreased everywhere by a factor of two. As can be noted from Fig. 4, the temperature of the core increases for a shorter period of time and to a significantly lesser extent than it did in simulation D1. Inspection of the data in Table 2 reveals that the inner core in this simulation is roughly 400 Myrs older than in simulation D1 and there is entropy available for ohmic dissipation for roughly 200 Myrs longer, due to the increased efficiency by which the mantle can cool off the core.

In Fig. 7 we show the results of simulation D4. This simulation is the same as D1 except that there is now 13 TW of internal heating throughout the mantle as well as a hot layer with 13 TW of internal heating at the base of the mantle as in D1. In contrast with runs D1 or D3, the CMB temperature increases for a significantly shorter period of time and thereafter decreases significantly more over the latter part of the simulation. This occurs because the extra heat sources in the mantle act both to increase the convective vigor in the mantle directly and they raise the temperature in the mantle, lowering the viscosity, which further leads to more vigorous mantle convection and efficient transport of heat to the Earth's surface. The final CMB temperature in this model is roughly 4000 K, which is close to the assumed value for this quantity. The plot in Fig. 7b reveals that the

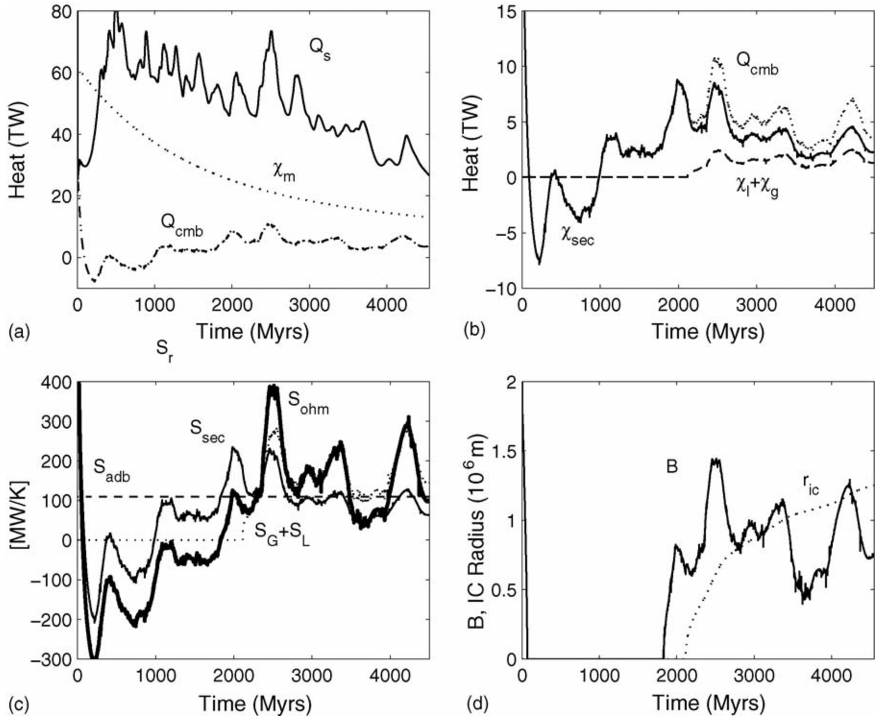

Fig. 7. From calculation D4: (a) mantle heat flows and sources; (b) core heat flows and sources; (c) entropy sources in the core; and (d) normalized magnetic field and the inner core radius.

heat is flowing from the mantle into the core for roughly the first 1 Gyrs of this simulation. There is no entropy available for ohmic dissipation for almost another 1 Gyr, however, as the CMB heat flow remains quite modest. In this case, the model geodynamo starts and remains active from a time just before the onset of inner core growth until the end of the simulation with a significant decrease in intensity around 3.6 Gyrs, correlated with fluctuations in mantle convection. Inspection of Fig. 7d reveals the sensitive response of the magnetic field to the mantle dynamics and the influence of the cooling history at the CMB on the rate of growth of the inner core. Furthermore, the magnetic field is relatively weak in this case since its onset is entirely correlated to the moment when the compositional terms enter the entropy budget and there was no thermally driven geodynamo prior to that. The liquidus temperature in the core is reached after approximately 2 Gyrs of evolution, yielding an older inner core, and it can be noted that the rate of growth is not constant, with an apparent faster growth of the inner core at the beginning. A varying regime for the inner core growth, also observed in other simulations, might be responsible for disturbing the hexagonal close-packing of the iron atoms, and possibly contributing to the inner core anisotropy (e.g., Tromp, 2001).

In Table 2 we also list the results of simulation H1, having the same total degree of radioactive internal heating as simulation D4, but where the internal heating has been uniformly distributed throughout the mantle. It can be seen that the CMB temperature decreases significantly more and the total entropy available for ohmic dissipation are significantly higher for this case. When the internal heat sources are uniformly distributed throughout the mantle, convection in the mantle is much more efficient, leading to much more rapid core cooling and at no time is the temperature of the lower mantle hotter than the temperature of the core. Simulation H1 does show significant temporal variations in the entropy available for dissipation as can be seen by the value of Σ_{ent} of 0.38.

In Fig. 8 we display the results of simulation D5 with only 4 TW of internal heating in the lowermost 200 km of the mantle in the final state and 13 TW distributed throughout the rest of the mantle. This calculation corresponds to the internal heating generated in the heterogeneous isotopic layer described in Tolstikhin and Hofmann (2005). The heat flows from the core into the mantle throughout the entire time of the simulation and as can be seen in Fig. 4, the CMB temperature drops by roughly 624 K over the time of the simulation. In this case, although the CMB heat flow remains positive,

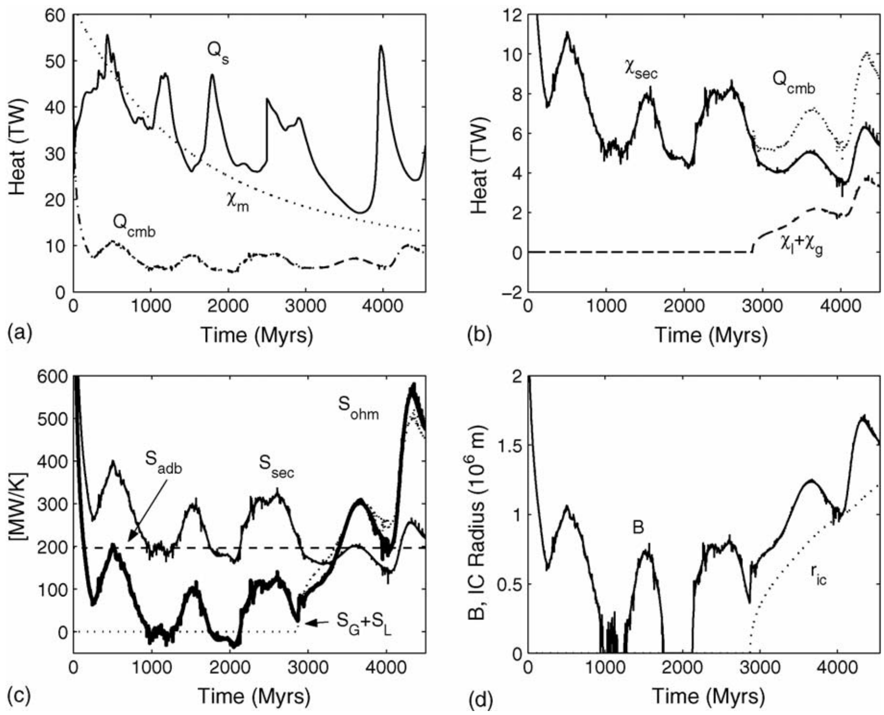

Fig. 8. From calculation D5: (a) mantle heat flows and sources; (b) core heat flows and sources; (c) entropy sources in the core; and (d) normalized magnetic field and the inner core radius.

it does drop to roughly 4 TW at times due to dynamical variations in convection in the mantle. During these CMB heat flow lows, before the onset of inner core growth, there is no entropy available for ohmic dissipation at times, and the model magnetic field vanishes. The magnetic field displays a high final value and also a higher variability than in the case B2, since its generation is related solely to the secular cooling term prior to the inner core freezing, and does not benefit from the more stabilizing regime given by the internal heating. It is worth noting that the degree of variability of the heat fluxes caused by mantle avalanches may be reduced if the simulations are performed in three dimensions (Tackley et al., 1993). Nonetheless, some features in the modeled magnetic field are found in the palaeomagnetic database, as for instance lower intensities at the early times (Macouin et al., 2004). An interesting observation that arises from this simulation is the fact that the apparent increase in the magnetic field intensity is starting before the onset of inner core crystallization, hence there is no absolute correlation between these two events.

3.4. Scaling of inner-core growth with time

In Table 2 we list the value of a parameter, α, which is calculated as the best fitting value in a least-squares sense for a model of inner core growth of the form $r = r_{\rm ic}^{p}\left(\frac{t-t^{\rm in}}{t^{p}-t^{\rm in}}\right)^{\alpha}$ where $r_{\rm ic}^{p}$ and t^{p} are the final inner core radius and time and $t^{\rm in}$ is the time of inner core growth initiation. A value of $\alpha = 0.5$ has been assumed in some previous work (e.g., Aurnou et al., 2003) for the scaling between the inner core radius and time. Inspection of Eq. (5) indicates that the inner core radius in our model scales like the square root of the difference between the liquidus temperature at the center of the Earth and the adiabatically extrapolated temperature at the CMB. As a result, if the core temperature decreases at a constant rate then α will be 0.5 while if the core secular cooling rate decreases over the lifetime of the inner core, α will be less than 0.5 which is the case in most of our simulations. This might be expected as the temperature difference between the core and mantle decreases with core cooling. There is no systematic variation in the value of α with the control parameters of the simulation, indicating that most of the variation in α is due to fluctuations in the dynamical simulation in the mantle for any particular simulation.

4. Discussion and conclusions

We have run a number of simulations of the Earth's thermal and magnetic evolution with various configurations of internal heating. The goal of the study has been to find models of the Earth's thermal evolution for which the final CMB temperature is in the range indicated by high pressure physics studies and the entropy available for ohmic dissipation is greater than zero throughout the latter 3500 Myrs of the simulation. It is also desirable if the entropy available for ohmic dissipation has not fluctuated too much over the course of a simulation. Our nominal simulation, B0, which starts with $T_{\mathrm{cmb}} = 4300\,\mathrm{K}$, with no internal heating in the core and homogeneous internal heating throughout the mantle, produces a magnetic field throughout its history but the final CMB temperature is quite low and the magnetic evolution features a high degree of variability in the magnetic field intensity.

Our model B2 with 300 ppm potassium in the core gives the magnetic field with the smallest temporal fluctuations. It also has a final CMB temperature that is within the bounds given by high pressure physics. This is in general agreement with the results of Nimmo et al. (2004), Labrosse (2003). In our calculations, the effects of increasing internal heating did not substantially increase the entropy available for dissipative processes since a great deal of the heat energy remained in the core and decreased the degree of secular cooling of the core. If convection in the mantle were more efficient, or if the temperature difference between the core and mantle were greater, then internal heating has a greater direct effect in increasing the entropy available for ohmic dissipation. There is a long standing debate in the geochemical and high pressure physics communities as to whether there can be significant quantities of potassium in the core (e.g., Chabot and Drake, 1999; Murthy et al., 2003; McDonough, 2004). If it emerges that it is possible that significant quantities of potassium are sequestered in the core, then internal heating in the core is an attractive scenario.

Various scenarios for layers with high internal heating at the base of the mantle exist. We have only examined the effects of a layer with a high degree of internal heating in direct contact with the core, as described in recent global geochemical models (Tolstikhin and Hofmann, 2005; Boyet and Carlson, 2005). Geodynamo simulations have also shown that Earth-like magnetic fields are best produced by models with roughly spatially uniform CMB heat flows which argues that any layer at the base of the mantle with a high degree of radio-active internal heating must be close to spatially homogeneous (Glatzmaier et al., 1999; Olson and Christensen, 2002). Most of our models with high degrees of internal heating at the base of the mantle have heat flowing from the mantle into the core for roughly the first two billion years of the simulation, a situation for which the operation of a geodynamo is clearly impossible. Even simulation D5, with a relatively modest 4 TW of internal heating in the lowermost layer, which did allow for heat flow from the core to the mantle throughout its history showed a magnetic field that vanished at times. We have shown, however, that if convection in the mantle is made more efficient by decreasing the viscosity of the mantle or by increasing the degree of internal heating in the mantle or if the initial core temperature is increased, it is possible to increase the degree of core cooling. Given the very high degree of heating in the very early Earth implied by radio-active decay in the hot basal layer, convection in the mantle would have to have been very efficient at early times in order to cause heat to flow from the core to the mantle. In such a case, a great deal of the Earth's early internal heat energy would be lost to the surface at early times which would make reconciling the Earth's relatively high current surface heat flow (Pollack et al., 1993) with geochemically constrained internal heating rates in the mantle (e.g., Hart and Zindler, 1986) more difficult. As such, with very careful tuning of the above mentioned parameters, a model may exist for which gradual cooling of the core occurs over the lifetime of the Earth leading to an old inner core and a magnetic field over the lifetime of the Earth due to a layer with high concentrations of radioactivity at the base of the mantle. Such a layer, representing an early-isolated, incompatible-element enriched reservoir is appealing from a geochemical standpoint. However, given the careful model tuning that it requires, it must be considered less likely from a geomagnetic perspective.

Acknowledgments

The authors wish to thank two anonymous reviewers who provided useful feed-back and greatly improved the quality of the manuscript. This work was funded by the Natural Sciences and Engineering Research Council of Canada.

References

Acuña, M.H., Connerney, J.E.P., Ness, N.F., Lin, R.P., Mitchell, D., Carlson, C.W., McFadden, J., Anderson, K.A., Reme, H., Mazelle, C., Vignes, D., Wasilewski, P., Cloutier, P., 1999. Global distribution of crustal magnetization discovered by the Mars Global Surveyor MAG/ER experiment. Science 284, 790–793.

Anderson, O.L., 2002. The power balance at the core-mantle boundary. Phys. Earth Plan. Int. 131, 1–17.

Aubert, J., 2005. Steady zonal flows in spherical shell dynamos. J. Fluid Mech. 542, 53–67.

Aurnou, J., Andreadis, S., Zhu, L.X., Olson, P., 2003. Experiments on convection in Earth's core tangent cylinder. Earth Plan. Sci. Lett. 212, 119–134.

Badro, J., Rueff, J-P., Vankó, G., Monaco, G., Fiquet, G., Guyot, F., 2004. Electronic Transitions in Perovskite: Possible Nonconvecting Layers in the Lower Mantle. Science 305, 383–386.

Boehler, R., 2000. High-pressure experiments and the phase diagram of mantle and core materials. Rev. Geophys. 38, 221–245.

Boyet, M., Carlson, R.W., 2005. ^{142}Nd Evidence for early ($>$ 4.53 Ga) Global Differentiation of the Sillicate Earth. Science 309, 576–581.

Braginsky, S.I., Roberts, P.H., 1995. Equations governing convection in Earth's core and the geodyanmo. Geophys. Astrophys. Fluid Dynam. 79, 1–97.

Brandon, A.D., Walker, R.J., Puchtel, I.S., Becker, H., Humayun, M., Revillon, S., 2003. ^{186}Os-^{187}Os systematics of the Gorgona Island komatiites: implication for early growth of the inner core. Earth Plan. Sci. Lett. 206, 411–426.

Breuer, D., Spohn, T., 2006. Viscosity of the Martian mantle and its initial temperature: constraints from crust formation history and the evolution of the magnetic field. Phys. Earth Plan. Int. 52, 153–169.

Buffett, B.A., Huppert, H.E., Lister, J.E., Woods, A.W., 1992. Analytical model for solidification of the earths core. Nature 356, 329–331.

Buffett, B.A., Huppert, H.E., Lister, J.E., Woods, A.W., 1996. On the thermal evolution of the Earth's core. J. Geophys. Res. 101, 7989–8006.

Buffett, B.A., 2003. The thermal state of Earth's core. Science 299, 1675–1677.

Buffett, B.A., 2002. Estimates of heat flow in the deep mantle based on the power requirements for the geodynamo. Geophys. Res. Lett. 29 (12), 7.

Butler, S.L., Peltier, W.R., 2000. On scaling relations in time-dependent mantle convection and the heat transfer constraint on layering. J. Geophys. Res. 105, 3175–3208.

Butler, S.L., Peltier, W.R., Costin, S.O., 2005. Numerical models of the Earth's thermal history: effects of inner-core solidification and core potassium. Phys. Earth Plan. Int. 152, 22–42.

Chabot, N.L., Drake, M.J., 1999. Potassium solubility in metal: the effects of composition at 15 kbar and 1900 C on partitioning between iron alloys and silicate melts. Earth Plan. Sci. Lett. 172, 323–335.

Christensen, U., Tilgner, A., 2004. Power requirements of the geodynamo from ohmic losses in numerical and laboratory dynamos. Nature 429, 169–171.

Coltice, N., Ricard, Y., 1999. Geochemical observations and one layer mantle convection Earth and Planetary Science Letters 174 (1–2), 125–137.

Costin, S.O., Buffett, B.A., Preferred reversal paths caused by a heterogeneuos conducting layer at the base of the mantle. J. Geophys. Res., 109, Art. No. B06101, 2004.

Gessmann, C.K., Wood, B.J., 2002. Potassium in the Earth's core? Earth Plan. Sci. Lett. 200, 63–78.

Glatzmaier, G.A., Coe, R.S., Hongre, L., Roberts, P.H., 1999. The role of the Earth's mantle in controlling the frequency of geomagnetic reversals. Nature 401, 885–890.

Gubbins, D., Alfe, D., Masters, G., Price, D.G., Gillan, M.J., 2003. Can the Earth's dynamo run on heat alone? Geophys. J. Int. 155, 609–622.

Hale, C.J., Dunlop, D.J., 1984. Evidence for an early Archean geomagnetic field; A paleomagnetic study of the Komati Formation, Barberton Greenstone Belt, South Africa. Geophys. Res. Lett. 11, 97–100.

Hale, C.J., 1987. The intensity of the geomagnetic field at 3.5 Ga: paleointensity results from the Komati Fomation, Barberton Mountain land, South Africa. Earth Plan. Sci. Lett. 86, 354–364.

Hart, S., Zindler, A., 1986. In search of a bulk-earth composition. Chem. Geol. 57, 247–267.

Heimpel, M.H., Aurnou, J.M., Al-Shamali, F.M., Gomez Perez, N., 2005. A numerical study of dynamo action as a function of spherical shell geometry. Earth Plan. Sci. Lett. 236, 542–557.

Keppler, H., Smyth, J.R., 2005. Optical and near infrared spectra of ringwoodite to 21.5 GPa: implications for radiative heat transport in the mantle. American Mineralogist 90, 1209–1212.

Kuang, W., Chao, B.F., 2003. Geodymano modelling and core-mantle interactions. In: Dehant, V., Creager, K.C., Karato, S., Zatman, S. (Eds.), Earth's Core: Dynamics, Structure, Rotation, AGU Geodymanics Series, 31., pp. 193–212.

Labrosse, S., Poirier, J.P., Le Mouël, J.-L., 2001. The age of the inner core. Earth Plan. Sci. Lett. 190, 111–123.

Labrosse, S., Macouin, M., 2003. The inner core and the geodynamo. Compt. Rend. Geosci. 335, 37–50.

Labrosse, S., 2003. Thermal and magnetic evolution of the Earth's core. Phys. Earth Plan. Int. 140, 127–143.

Lay, T., Williams, Q., Garnero, E.J., 1998. The core-mantle boundary layer and deep Earth dynamics. Nature 392, 461–468.

Lee, K., Jeanloz, R., 2003. High-pressure alloying of potassium and iron: Radioactivity in the Earth's core? Geophys. Res. Lett. 30 (23).

Lister, J.R., 2003. Expressions for the dissipation driven by convection in the Earth's core. Phys. Earth Plan. Int. 140, 145–158.

Lister, J.R., Buffett, B.A., 1995. The strength and efficiency of the thermal and compositional convection in the geodynamo. Phys. Earth Plan. Int. 91, 17–30.

Macouin, M., Valet, J.-P., Besse, J., 2004. Long term evolution of the geomagnetic dipole moment. Phys. Earth Plan. Int. 147, 239–246.

McDonough, W.F., 2004. Compositional Model for the Earth's Core. In: Carlson, R.W., Holland, H.D., Turekian, K.K. (Eds.), Treatise on Geochemistry: The Mantle and Core, Vol. 2. Elsevier, Oxford, pp. 547–569.

McElhinny, M.W., Senanayake, W.E., 1980. Paleomagnetic evidence for the existence of the geomagnetic field 3.5 Ga ago. J. Geophys. Res. 85, 3523–3528.

Murthy, V.M., van Westrenen, W., Fei, Y.W., 2003. Experimental evidence that potassium is a substantial radioactive heat source in planetary cores. Nature 423, 163–165.

Nakagawa, T., Tackley, P.J., 2005. Deep mantle heat flow and thermal evolution of the Earth's core in thermochemical multiphase models of the mantle. Geochem. Geophys. Geosyst. 6 doi:10.1029/2005GC000967.

Nimmo, F., Price, G.D., Brodholt, J., Gubbins, D., 2004. The influence of potassium on core and geodynamo evolution. Geophys. J. Int. 156, 363–376.

Nimmo, F., 2002. Why does Venus lack a magnetic field? Geology 30, 987–990.

Olson, P.L., Aurnou, J.M., 1999. A polar vortex in the Earth's core. Nature 402, 170–173.

Olson, P.L., Christensen, U., 2002. The time-averaged magnetic field in numerical dynamos with non-uniform boundary heat flow. Geophys. J. Int. 151, 809–823.

Pollack, H.N., Hunter, S.J., Johnson, J.R., 1993. Heat flow from the Earth's interior: analysis of the global data set. Rev. Geophys. 31, 267–280.

Prévot, M., Derder, M.E., McWilliams, M., Thompson, J., 1990. Intensity of the Earth's magnetic field: evidence for a Mesosoic dipole low. Earth Plan. Sci. Lett. 97, 129–139.

Russell, S.A., Lay, T., Garnero, E.J., 1998. Seismic eveidence for the small-scale dynamics in the lowermost mantle at the root of the Hawaiian spot. Nature 396, 255–258.

Smirnov, A.V., Tarduño, J.A., Pisaken, B.N., 2003. Paleointensity of the early geodynamo (2.45 Ga) as recorded in Karelia: a single-crystal approach. Geology 31, 415–418.

Solheim, L., Peltier, W.R., 1994a. Avalanche effects in phase transition modulated thermal convection: a model of the Earth's mantle. J. Geophys. Res. 99, 6997–7018.

Solheim, L., Peltier, W.R., 1994b. Phase boundary deflections at 660 km depth and episodically layered isochemical convection in the mantle. J. Geophys. Res. 99, 15861–15875.

Stacey, F.D., 1992. Physics of the Earth, third ed. Brookfield Press, Brisbane, Australia.

Steinbach, V., Yuen, D.A., Zhao, W., 1993. Instabilities from phase transitions and the timescales of mantle thermal evolution. Geophys. Res. Lett. 20, 1119–1122.

Stegman, D.R., Jellinek, A.M., Zatman, S.A., Baumgardner, J.R., Richards, M.A., 2003. An early lunar core dynamo driven by thermochemical mantle convection. Nature 421, 143–146.

Stevenson, D.J., 2003a. Planetary magnetic fields. Earth Plan. Sci. Lett. 208, 1–11.

Stevenson, D.J., 2003b. Styles of mantle convection and their influence on planetary evolution. Compt. Rend. Geosci. 335, 99–111.

Stieglitz, R., Müller, U., 2001. Experimental demonstration of the homogeneous two-scale dynamo. Phys. Fluids 13, 561–564.

Tackley, P.J., Stevenson, D.J., Glatzmaier, G.A., Schubert, G., 1993. Effects of an endothermic phase transition at 670 km depth in a spherical model of convection in the Earth's mantle. Nature 361, 699–704.

Tanaka, H., Kono, M., Uchimura, H., 1995. Some global features of palaeointensity in the geological time. Geophys. J. Int. 120, 97–102.

Tolstikhin, I., Hofmann, A.W., 2005. Early crust on top of the Earth's core. Phys. Earth Plan. Int. 148, 109–130.

Tromp, J., 2001. Inner-core anisotropy and rotation. Ann. Rev. Earth Planet. Sci. 29, 47–69.

Williams, Q., Garnero, E.J., 1996. Seisminc evidence for partial melt at the base of the Earth's mantle. Science 273, 1528–1530.